

A study on the preparation, evaluation of biological characteristics, and preliminary imaging of [^{188}Re]Re-ibandronate

Tingting Xu

Luzhou Medical College: Southwest Medical University

Yingwei Wang

Luzhou Medical College: Southwest Medical University

Zan Chen

Luzhou Medical College: Southwest Medical University

Hanxiang Liu

Luzhou Medical College: Southwest Medical University

Songsong Yang

Luzhou Medical College: Southwest Medical University

Guangfu Liu

Luzhou Medical College: Southwest Medical University

Yan Zhao

Luzhou Medical College: Southwest Medical University

Wenhui Fu

Luzhou Medical College: Southwest Medical University

Lin Liu

Luzhou Medical College: Southwest Medical University

Ke Xiang

Luzhou Medical College: Southwest Medical University

Dengsai Peng

Luzhou Medical College: Southwest Medical University

Yue Chen (✉ chenyue5523@126.com)

<https://orcid.org/0000-0003-4088-7649>

Original research

Keywords: 188Re, ibandronate, radiolabeling, biological characteristics, bone imaging

Posted Date: February 23rd, 2021

DOI: <https://doi.org/10.21203/rs.3.rs-236688/v1>

License: © ⓘ This work is licensed under a Creative Commons Attribution 4.0 International License. [Read Full License](#)

Abstract

Background

Bone is a common site of metastasis of malignant tumor. Several radiopharmaceuticals are available to relieve bone pain in patients with cancer. However, there is still a need to investigate easily accessible and high bone affinity radiopharmaceuticals. Radionuclide ^{188}Re has an advantage in this regard because of its commercial extraction from $^{188}\text{W}/^{188}\text{Re}$ generators. It can be used on demand and is cost-effective. The first-generation bisphosphonate hydroxyethylidene diphosphonate (HEDP) is the commonly used bisphosphonate for ^{188}Re -labelling. And the third-generation bisphosphonates ibandronate (IBA) has higher bone affinity and ability to inhibit bone resorption than HEDP. However, there have been no reports on ^{188}Re -labelling with IBA. We used IBA and ^{188}Re for radiolabeling to develop and evaluate a novel type of bone-seeking radiopharmaceutical.

Results

We successfully prepared $[^{188}\text{Re}]\text{Re-IBA}$ in >95% RCP. The optimum preparation conditions were as follows: IBA, 1.2–1.6 mg; ascorbic acid, 0.20–0.35 mg; stannous chloride, 0.14–0.18 mg; potassium perrhenate, 0.005–0.009 mg; and $[^{188}\text{Re}]\text{ReO}_4^-$ activity, 18.5–55 MBq, were reacted for 30 min at 95°C and pH = 2. $[^{188}\text{Re}]\text{Re-IBA}$ demonstrated good stability in vitro, high plasma protein binding rate, and good hydrophilicity. The in vivo distribution of mice and bone imaging in New Zealand rabbits showed high bone uptake, long retention time, rapid blood clearance, and relatively low soft tissue uptake.

Conclusion

Our study encompassed the successful preparation of $[^{188}\text{Re}]\text{Re-IBA}$, a novel bone-seeking radiopharmaceutical, and confirmed it has great potential for the treatment of bone pain and imaging monitoring.

Introduction

Bone is a common site of metastasis of malignant tumor. Up to 80% and 50% of the patients with prostate cancer and breast cancer, respectively, have bone metastasis[1, 2]. The risk of bone metastasis in patients with lung, thyroid, and kidney cancer is about 30–40%[3, 4]. Patients with bone metastasis usually experience severe and refractory pain. Furthermore, it may be accompanied by pathological fractures, spinal cord compression, hypercalcemia, and other complications, thus seriously affecting the quality of life[5]. Therefore, a timely and effective treatment is needed to alleviate the symptoms and improve the quality of life.

The currently available treatments for bone metastasis are chemotherapy, radiotherapy, bisphosphonate therapy, hormone therapy, and the use of painkillers[5]. However, the aforementioned methods have some limitations[6]. The use of bone-seeking radiopharmaceuticals is another effective method to relieve bone pain. It has the advantages of simultaneous treatment of multiple metastases, repeatability, and combination with other treatments[7]. Moreover, it can reduce or postpone the incidence of skeletal-related events[8]. There are several radionuclides available for bone-targeted radionuclide therapy, including ^{89}Sr , ^{153}Sm , ^{186}Re , ^{188}Re , ^{177}Lu , and ^{223}Ra [6, 9]. ^{89}Sr and ^{223}Ra are calcium mimetic radionuclides. They have natural tropism for the bone, which

enables the deposition of hydroxyapatite in the bones[10]. While ^{89}Sr releases β^- rays, ^{223}Ra treats bone lesions by releasing α particles. Both are primarily used in the form of chloride ($[^{89}\text{Sr}]\text{SrCl}_2$ and $[^{223}\text{Ra}]\text{RaCl}_2$). In contrast, ^{153}Sm , ^{186}Re , ^{188}Re , and ^{177}Lu do not have natural tropism for the bone. This necessitates their radiolabeling with bisphosphonates. The major forms of ^{153}Sm , ^{186}Re , ^{188}Re , and ^{177}Lu include $[^{153}\text{Sm}]\text{Sm}$ -ethylenediamine tetramethylene phosphonate ($[^{153}\text{Sm}]\text{Sm}$ -EDTMP), $[^{186}\text{Re}]\text{Re}$ -hydroxyethylidene diphosphonate ($[^{186}\text{Re}]\text{Re}$ -HEDP), $[^{188}\text{Re}]\text{Re}$ -HEDP, and $[^{177}\text{Lu}]\text{Lu}$ -EDTMP, respectively. The aforementioned bisphosphonate-labeled radiopharmaceuticals can be combined with hydroxyapatite crystals for deposition in the bones, particularly in areas with an active osteogenic reaction. The bone lesions are subsequently treated by releasing β^- rays.

Despite the diversity of options, commercially available radiopharmaceuticals are limited. Most of the radionuclides used for the treatment are produced through reactors, thus are extremely expensive. The radionuclide ^{188}Re has an advantage owing to its availability from commercial $^{188}\text{W}/^{188}\text{Re}$ generators. It can be used on demand and is cost-effective. ^{188}Re has a physical half-life of 16.9 h and can produce β^- rays with a maximum energy of 2.1 MeV for treatment[11]. It also emits γ rays with an energy of 155 keV for imaging, which facilitates visualizing the distribution of radioactive tracers in the body during treatment[11]. $[^{188}\text{Re}]\text{Re}$ -HEDP is one of the most widely used bisphosphonate radiopharmaceuticals in clinical nuclear medicine that relieves bone pain caused by prostate cancer, breast cancer, or other tumors[12]. However, there is a need to identify bisphosphonates with stronger bone-targeting ^{188}Re -compound. Bisphosphonates are analogues of endogenous pyrophosphates, characterized by P-C-P bonds. They comprise a hydroxyl group in one position of the carbon, which has a high affinity for calcium phosphate, the primary mineral of the bone[13]. Moreover, it comprises a side chain structure that inhibits bone resorption in the other position of the carbon[13]. The side chain structure of the first-generation bisphosphonate does not contain nitrogen. HEDP is one of its representative drugs. In contrast, the side-chain structure of the second and third-generation bisphosphonates contains nitrogen. Furthermore, the third-generation bisphosphonate side chain also contains a heterocyclic structure and its ability to inhibit bone resorption is significantly stronger than that of the first- and second-generation bisphosphonates. However, nitrogen-containing bisphosphonates may have significant side effects, including renal failure, hypocalcemia, and osteonecrosis of the jaw[14]. The choice of drugs with lower toxicity is an important factor in determining the treatment of patients with renal insufficiency. Ibandronic acid and zoledronic acid are the most powerful and widely used third-generation bisphosphonates. Studies[15, 16] on the effects of the aforementioned bisphosphonates on renal safety have reported on the possible occurrence of nephrotoxicity while using zoledronic acid. Nonetheless, the nephrotoxicity of ibandronic acid is extremely low and is equivalent to placebo. Another study [17]conducted on 44 patients treated with ibandronate (IBA) reported no impairment of renal function during an average follow-up of 18.5 months. In addition, Han et al. [18]mentioned that the pain relief rate and improvement in the quality of life in patients with bone tumor were higher in the ibandronic acid group than the zoledronic acid group ($P < 0.05$). Nonetheless, the rate of adverse reaction was lower in the ibandronic acid group than in the zoledronic acid group ($P < 0.05$). There have been no reports on ^{188}Re -labelling with IBA. Therefore, we selected IBA and ^{188}Re for radiolabeling to develop and evaluate a new type of radiopharmaceutical with potential bone-seeking properties and low toxicity, which may contribute to individualized treatment in the era of precision medicine. We will shed light on the preparation, optimization of conditions, biological evaluation, and preliminary imaging studies of $[^{188}\text{Re}]\text{Re}$ -IBA in detail.

Materials And Methods

Materials

[¹⁸⁸Re]NaReO₄ was eluted from the alumina based ¹⁸⁸W/¹⁸⁸Re generator (OncoBeta, Germany) with saline solution (0.9% NaCl). We purchased IBA from Twbio Technology Co., Ltd., Beijing, China. Ascorbic acid, potassium perrhenate (KReO₄), and stannous chloride (SnCl₂) were purchased from Macklin Biochemical Co., Ltd., Shanghai, China. All the aforementioned reagents can be directly used without further purification. We used Xinhua No. 1 chromatography paper (Xinhua Paper Industry Co., Ltd., Hangzhou, China) for paper chromatography (PC). Moreover, the distribution of radioactivity on the PC strips was measured by a thin-layer chromatographic (TLC) scanner (Bioscan Inc, Washington, DC, USA). We used a dose calibrator (CRC-25R; Hengyide Technology Co., Ltd., Beijing, China) and a gamma counter (SN-695B; Hesuo Rihuan Photoelectric Instrument Co, Shanghai, China) to measure the radioactivity of the samples. Bone imaging was performed by single photon emission computed tomography (SPECT; GE infinia T4, GE, USA). Furthermore, we purchased Kunming mice and New Zealand white rabbits from the Animal Experiment Center, Southwest Medical University, Luzhou, Sichuan, China. Other equipment and chemicals used in the experiment were provided by the Nuclear Medicine and Molecular Imaging Key Laboratory of Sichuan Province. All studies were approved by the Ethics Committee of Southwest Medical University.

Methods

1 Radiolabeling

We determined the effects of IBA, ascorbic acid, KReO₄, SnCl₂, [¹⁸⁸Re]ReO₄⁻ activity, pH, temperature, and reaction time on the RCP of [¹⁸⁸Re]Re-IBA by the method of controlled variables. First, we prepared IBA, ascorbic acid, and KReO₄ into solutions of 30 mg/ml, 50 mg/ml and 0.2 mg/ml, respectively. SnCl₂ was prepared into a solution of 6 mg/ml with 0.1 N hydrochloric acid. Moreover, we controlled the activity of [¹⁸⁸Re]ReO₄⁻ eluent as 370 MBq/ml. We sequentially mixed 0.2–4.0 mg, 0–0.5 mg, 0.02–0.4 mg, and 0–0.019 mg of IBA, ascorbic acid, SnCl₂, and KReO₄, respectively. We then added the fresh eluted [¹⁸⁸Re]ReO₄⁻ solution. Subsequently, we adjusted the pH value to 0.5–9 with 1 N sodium acetate solution and 1 N hydrochloric acid. The reaction occurred at temperatures of room temperature (25±2°C), 60°C, and 95°C for 10–60 min, respectively. After the reaction was completed, it was cooled to room temperature (25±2°C). The pH value of each tube was adjusted to 6–7. We used an aseptic filter membrane of 0.22 μm for sterilization and filtration.

2 Quality control

The RCP of [¹⁸⁸Re]Re-IBA was determined by TLC. The method of radioactivity quantification involved cutting the chromatography paper into 2 cm wide and 15 cm long PC strips. We used a pencil to draw a straight line, 2 cm away from one end of the strips to mark the origin. We eventually added 3–5 μL of the final solution at the origin of the strips. We used acetone and saline as the solvents. A TLC scanner was used to measure the distribution of radioactivity on the PC strips. We calculated the RCP of [¹⁸⁸Re]Re-IBA from the peak area measurements as follows:

$$\text{RCP} = 100\% - (\% [^{188}\text{Re}]\text{ReO}_4^- + \% [^{188}\text{Re}]\text{ReO}_2).$$

3 In vitro stability

Two test tubes were labeled No. 1 and No. 2. While we added 0.1 ml of normal saline in No. 1, 0.1 ml of fresh human serum, diluted 10 times, was added to No. 2. We incubated the tubes with freshly prepared 37 MBq [^{188}Re]Re-IBA under the best labeling conditions. While No. 1 was placed at room temperature ($25\pm 2^\circ\text{C}$), No. 2 was incubated at 37°C . We determined the RCP of the tubes by TLC at 30 min, 1 h, 3 h, 6 h, 8 h, and 24 h. We repeated the experiment thrice. The results are expressed as mean \pm standard deviation ($\bar{x}\pm s$).

4 Plasma protein binding rate

Fresh human plasma was prepared with 1 ml heparin. Three test tubes were numbered A1, A2, and A3. We added 0.1 ml fresh human plasma and freshly prepared 1.85 MBq [^{188}Re]Re-IBA to them under the best labeling conditions and incubated them at 37°C for 2 h. We then added 1 ml of 25% trichloroacetic acid solution to each test tube and centrifuged them at 2000 r/min for 5 min. The supernatant for A1, A2, and A3 was collected into three corresponding test tubes labeled B1, B2, and B3, respectively. The centrifugation was repeated and the supernatant was collected thrice. We used the γ counter to measure the radioactivity counts of precipitate in the A tubes and supernatant in the B tubes. The plasma protein binding rate (PPB) was calculated as follows:

$$\text{PPB} = [(A - \text{background}) / (A + B - \text{background} \times 2)] \times 100\%$$

The result is expressed as mean \pm standard deviation ($\bar{x}\pm s$).

5 Lipids and water distribution coefficient

Three 5 ml test tubes were numbered A1, A2, and A3. We added freshly prepared 1.85 MBq [^{188}Re]Re-IBA to each tube under optimal labeling conditions. Each test tube was shaken for 20 min with a vortex mixer, followed by centrifugation at 2000 r/min for 5 min. The upper liquid (organic phase) 0.1 ml was collected into three test tubes (numbered B1, B2, and B3). Moreover, the lower liquid (water phase) 0.1 ml was collected into three test tubes (numbered C1, C2, and C3). The radioactivity counts of organic phase and water phase were measured by a γ counter. Furthermore, the lipid-water partition coefficient ($\lg p$) was calculated by using the formula as follows:

$$\lg p = \lg [(B - \text{background}) / (C - \text{background})]$$

The results are expressed as mean \pm standard deviation ($\bar{x}\pm s$).

6 The in vivo distribution of [^{188}Re]Re-IBA and [^{188}Re]ReO $_4^-$

Twenty-four Kunming mice, aged 4–5 weeks (roughly 18–22 g) were randomly divided into six groups, with four mice in each group (equal number of males and females). Each group was injected with [^{188}Re]Re-IBA 3.7 MBq (0.1 ml) through the tail vein. Following the injection, we sacrificed the mice by CO $_2$ asphyxiation at 1 h, 3 h, 6 h, 8 h, 24 h, and 48 h. We collected the blood samples by cardiac puncture. The tissues of the heart, liver, spleen, lung, kidney, stomach, small intestine, brain, femur, muscles, and gonad were removed, washed, and weighed. Moreover, we used a γ counter to measure the radioactivity count. Following the time attenuation correction, we calculated the percentage injection dose rate per gram of tissue (% ID/g) at each time point. The result is expressed as mean \pm standard deviation ($\bar{x}\pm s$). We studied the in vivo distribution of [^{188}Re]ReO $_4^-$ using the aforementioned method.

7 Imaging of New Zealand Rabbits with [^{188}Re]Re-IBA

We used New Zealand rabbits, weighing about 2.5 kg in this study. Following an intraperitoneal injection of 2% pentobarbital sodium (40 mg/kg), the rabbits were fixed after anesthesia. We injected [¹⁸⁸Re]Re-IBA 100 MBq (0.5 ml) through the marginal ear vein. Dynamic bone imaging was performed within 20–120 min after the injection. Moreover, we performed whole-body bone static imaging at 3 h, 4 h, 6 h, 8 h, 24 h, and 48 h (acquisition equipment: American GE infinia T4 double probe SPECT instrument, high energy collimator; scanning parameters: energy peak- 155KeV, posture- supine position, head advanced, matrix- 128 × 128, and window width- ±10%). Following the image acquisition, we processed them by using the software of the post-processing workstation.

Results

1 Radiolabeling and quality control

We studied various reaction parameters by using control variables to determine the optimal conditions for the production of [¹⁸⁸Re]Re-IBA. The optimum preparation conditions were as follows: IBA, 1.2–1.6 mg; ascorbic acid, 0.20–0.35 mg; SnCl₂, 0.14–0.18 mg; KReO₄, 0.005–0.009mg; and [¹⁸⁸Re]ReO₄⁻ activity, 18.5–55 MBq. They were reacted for 30min at 95 °C and pH = 2. We used TLC for RCP analysis. Fig. 1 and 2 outline the effects of various variables on the RCP of [¹⁸⁸Re]Re-IBA. Upon using acetone as an eluting solvent, the colloidal impurity [¹⁸⁸Re]ReO₂ and product [¹⁸⁸Re]Re-IBA remain at the origin of PC strip. However, [¹⁸⁸Re]ReO₄⁻ moves with the solvent front. In contrast, upon using saline as the eluting solvent, the colloidal impurity [¹⁸⁸Re]ReO₂ remains at the origin, while [¹⁸⁸Re]ReO₄⁻ and product [¹⁸⁸Re]Re-IBA move with the solvent front. [¹⁸⁸Re]Re-IBA could be consistently prepared in >95% RCP under the best preparation conditions. Moreover, it did not require further purification.

2 In vitro stability

We measured the stability of the markers in normal saline and serum at room temperature (25±2°C) and 37 °C, respectively. Table 1 summarizes the results. [¹⁸⁸Re]Re-IBA placed in saline at room temperature (25±2°C) demonstrated good in vitro stability. The RCP was >95% and >90% at 8 h and 24 h, respectively. The stability of [¹⁸⁸Re]Re-IBA placed in serum at 37°C was slightly lower than that placed in saline at room temperature (25±2°C). Nonetheless, the overall stability was good.

Table 1. The in vitro stability of [¹⁸⁸Re]Re-IBA under different methods and time

	30 min (%)	1 h (%)	3 h (%)	6 h (%)	8 h (%)	24 h (%)
Room temperature (25±2°C), normal saline	98.64±0.4	97.44±0.7	97.07±0.7	96.43±0.9	95.54±0.8	93.33±0.5
37°C, serum	98.73±0.4	97.47±0.8	96.86±0.9	95.32±2.5	90.30±2.3	83.11±0.7

3 Plasma protein binding rate

We evaluated the PPB of the marker by the abovementioned method. The PPB of [¹⁸⁸Re]Re-IBA incubated in plasma for 2 h was 79 ±0.71% under optimum labeling conditions.

4 Lipids and water distribution coefficient

The IgP of the marker was evaluated by the above-mentioned method. The IgP of $[^{188}\text{Re}]\text{Re-IBA}$ was -2.33 ± 0.02 under optimum labeling conditions, which indicated high hydrophilia.

5 | The in vivo distribution of $[^{188}\text{Re}]\text{Re-IBA}$ and $[^{188}\text{Re}]\text{ReO}_4^-$

Table 2 and 3 summarize the in vivo distribution of $[^{188}\text{Re}]\text{Re-IBA}$ and $[^{188}\text{Re}]\text{ReO}_4^-$ in mice. In table 2, we observed a rapid blood clearance of $[^{188}\text{Re}]\text{Re-IBA}$. Moreover, the blood uptake was 0.622 ± 0.103 %ID/g and 0.049 ± 0.016 %ID/g at 3 h and 24 h, respectively. The bone uptake of $[^{188}\text{Re}]\text{Re-IBA}$ was high, and the %ID/g reached the maximum at 6 h (10.394 ± 3.849 %ID/g). This was followed by a decrease in the bone uptake with time. Nonetheless, the percentage injection dose rate per gram tissue was still as high as 5.699 ± 1.331 %ID/g at 48 h. This in turn was significantly higher than that in other organs and tissues. In addition, the radioactivity ratio of the bone to the heart, liver, blood, and muscles was highest at 48 h, which were 327.902, 111.183, 326.053, and 291.551, respectively. The highest uptake occurred in the kidneys except the bone, which is related to the kidney as the primary excretory organ. We could observe the distribution of radioactivity in the stomach within 8 h. However, the gastric uptake gradually decreased with time. Table 3 outlines the distribution of $[^{188}\text{Re}]\text{ReO}_4^-$ in mice. The highest uptake of $[^{188}\text{Re}]\text{ReO}_4^-$ occurred in the stomach between 1–8 h. The uptake in the blood, lungs, and kidney was also higher. However, the uptake was low in the bone. Furthermore, the radioactivity ratio of bone to the heart, liver, blood, and muscle was low. The highest ratio was as low as 2.372 (bone/muscle, 8 h).

6 | Imaging of New Zealand Rabbits with $[^{188}\text{Re}]\text{Re-IBA}$

Fig. 3 and 4 depicts the dynamic bone imaging for 20–120 min and whole-body bone static imaging of 3–48 h in the New Zealand rabbits, following an injection of 100 MBq $[^{188}\text{Re}]\text{Re-IBA}$. There was an obvious accumulation in both kidneys, bladder, and bones 20 min after the injection. As time goes on, the accumulation in the kidneys gradually faded and got excreted with urine; furthermore, the soft tissue accumulation gradually faded and disappeared; the whole-body bone imaging was clear with a high contrast between the bone and the background, which consistent with the in vivo distribution in mice.

Discussion

Numerous radiopharmaceuticals have been used to target and relieve bone pain since the introduction of radionuclides to treat bone pain in the 1940s[19]. Several radiopharmaceuticals are available to relieve bone pain in patients with cancer, including $[^{89}\text{Sr}]\text{SrCl}_2$, $[^{153}\text{Sm}]\text{Sm-EDTMP}$, $[^{186}\text{Re}]\text{Re-HEDP}$, $[^{188}\text{Re}]\text{Re-HEDP}$, $[^{177}\text{Lu}]\text{Lu-EDTMP}$, and $[^{223}\text{Ra}]\text{RaCl}_2$ [6, 9]. However, each radiopharmaceutical has its own advantages and disadvantages. The choice is extremely dependent on the patient's status, such as the renal function and bone marrow reserve, cancer extent (extraskelatal lesions and the bulk of the tumor), and physical properties of radionuclides[19]. As the commercial availability of radiopharmaceuticals is limited, the availability of each radiopharmaceutical also needs to be considered. Moreover, most of the radionuclides used for treatment are produced through reactors, thus are extremely expensive. Therefore, it is important to choose an easily accessible and cost-effective radiopharmaceutical. Radionuclide ^{188}Re has an advantage in this regard because of its commercial extraction from $^{188}\text{W}/^{188}\text{Re}$ generators, which can be used on demand. Moreover, it is cost-effective. The first-generation bisphosphonate HEDP is the commonly used bisphosphonate for ^{188}Re -labelling. It has lower bone affinity and ability to inhibit bone resorption than the third-generation bisphosphonates IBA and is zoledronic acid. In addition,

the rate of adverse reactions, including nephrotoxicity of IBA is lower than that of zoledronic acid[15, 16, 18]. We selected IBA and ^{188}Re for radiolabeling was based on the unique advantages of ^{188}Re in palliative treatment of metastatic bone pain and the low toxicity of IBA.

Previous studies [20] have identified ascorbic acid as the best antioxidant in $[^{188}\text{Re}]\text{Re}$ -bisphosphonate, which is better than gentian acid and citric acid. Therefore, we use ascorbic acid as the antioxidant. In addition, we chose SnCl_2 as the reducing agent to reduce $[^{188}\text{Re}]\text{ReO}_4^-$ to a lower oxidation state and facilitate its reaction with IBA. However, an insufficient amount of SnCl_2 will lead to the production of unreduced free $[^{188}\text{Re}]\text{ReO}_4^-$. Furthermore, its excessive use might form $[^{188}\text{Re}]\text{ReO}_2$ colloids in the product. Therefore, it is necessary to ensure the best ratio of SnCl_2 with IBA and $[^{188}\text{Re}]\text{ReO}_4^-$. The ^{188}Re obtained in the generator was carrier-free. Hence, we added KReO_4 as a carrier to ensure the labeling efficiency and stability. In previous studies[21–28], $[^{188}\text{Re}]\text{Re}$ -bisphosphonate, without a carrier, has a low labeling rate, poor stability, unusually high soft tissue activity, and little bone uptake. Our findings also confirmed the difference of RCP in conditions, with and without proper amount of KReO_4 (RCP < 80% vs RCP > 95%).

The stability of radiopharmaceuticals is extremely important for therapy. Following the preparation of $[^{188}\text{Re}]\text{Re}$ -IBA at room temperature ($25 \pm 2^\circ\text{C}$) and placing it in normal saline for 24 h, the RCP was > 95% at 8 h, thus confirming its safe placement and use. In addition, the PPB of $79 \pm 0.71\%$ suggested that the $[^{188}\text{Re}]\text{Re}$ -IBA is a radiopharmaceutical with a higher protein binding rate. It predominantly binds to the protein in the body and can maintain its pharmacological effect for a long time.

Radiopharmaceuticals should achieve ideal therapeutic effects and minimize related toxicity to gain efficacy as therapeutic drugs[6]. $[^{188}\text{Re}]\text{Re}$ -IBA showed a rapid blood clearance rate and the blood uptake was almost undetectable at 24 h. Despite the elimination of most of the $[^{188}\text{Re}]\text{Re}$ -IBA activity through the kidney, its bone uptake was high and the soft tissue uptake was low, with a high target/non-target (T/NT) ratio. The in vivo distribution of $[^{188}\text{Re}]\text{ReO}_4^-$ revealed that the free $[^{188}\text{Re}]\text{ReO}_4^-$ was poorly targeted to the bone. Thus confirming the success and bone-targeting capability of the labeled $[^{188}\text{Re}]\text{Re}$ -IBA. The imaging results of New Zealand rabbits further revealed high uptake and long retention time of $[^{188}\text{Re}]\text{Re}$ -IBA in the bone. And its soft tissue clearance was fast, and non-target tissue uptake was low. Moreover, the overall image quality was good. Hence, $[^{188}\text{Re}]\text{Re}$ -IBA has great potential for the treatment of bone pain, and it also can be used for therapeutic imaging monitoring. In addition, we observed radioactivity of $[^{188}\text{Re}]\text{Re}$ -IBA in the mice gastric mucosa within 8 h. We initially considered the gastric uptake to be a consequence of $[^{188}\text{Re}]\text{Re}$ -IBA catabolism which releases $[^{188}\text{Re}]\text{ReO}_4^-$. However, other ^{188}Re -compounds, including $[^{188}\text{Re}]\text{Re}$ -HEDP also showed higher gastric uptake at an early stage in mice[21, 29, 30]. Park et al. [30] postulated the high uptake of ^{188}Re -compound in the stomach to be related to the acidic environment in the stomach of mice rather than an outcome of catabolism. In our study, we obtained satisfactory results of in vitro stability. Moreover, the imaging of the New Zealand rabbits did not show high gastric uptake. It is unclear whether $[^{188}\text{Re}]\text{Re}$ -IBA had partial catabolism in mice or was specifically ingested in the stomach of mice. However, both cases showed differences in the characteristics of $[^{188}\text{Re}]\text{Re}$ -IBA compared to those observed in the New Zealand rabbits, thus necessitating further study.

Conclusion

This study encompassed the successful preparation of [^{188}Re]Re-IBA, a novel bisphosphonate radiopharmaceutical. The aforementioned radiopharmaceutical has the advantages of a simple preparation method, high stability, plasma protein binding rate, and good hydrophilicity. The in vivo biological distribution in mice and imaging of New Zealand rabbits confirmed the following: rapid blood clearance, high affinity to the bone, long retention time in the bone, high T/NT ratio, and low uptake in the liver, spleen, and soft tissue. Therefore, [^{188}Re]Re-IBA is a suitable candidate for bone-targeted therapy and has an excellent performance. It has great potential for the treatment of bone pain and monitoring the therapeutic effects. However, researchers should explore animal models of metastatic bone tumor to completely clarify the therapeutic effects and value of [^{188}Re]Re-IBA.

Abbreviations

HEDP: Bisphosphonate hydroxyethylidene diphosphonate

IBA: Ibandronate

RCP: Radiochemical purity

SPECT: Single photon emission computed tomography

EDTMP: Ethylenediamine tetramethylene phosphonate

PC: Paper chromatography

TLC: Thin-layer chromatographic

Declarations

Ethics approval and consent to participate: All studies were approved by the Ethics Committee of Southwest Medical University.

Consent for publication: Not applicable.

Availability of data and material: The datasets and materials during the present study are available from the corresponding author on reasonable request.

Competing interests: The authors declare that they have no competing interests.

Funding: Project 81671721 supported by National Natural Science Foundation of China.

Authors' contributions: TX, YW, and ZC contributed equally to this work and shared joint first authorship.

Acknowledgements: We would like to thank Editage (www.editage.com) for English language editing.

References

1. Chow E, Meyer RM, Ding K, et al. Dexamethasone in the prophylaxis of radiation-induced pain flare after palliative radiotherapy for bone metastases: a double-blind, randomised placebo-controlled, phase 3 trial.

- Lancet Oncol. 2015;16:1463-1472.
2. Gdowski AS, Ranjan A, Vishwanatha JK, et al. Current concepts in bone metastasis, contemporary therapeutic strategies and ongoing clinical trials. *J Exp Clin Cancer Res.* 2017;36:108.
 3. Paes FM, Serafini AN. Systemic Metabolic Radiopharmaceutical Therapy in the Treatment of Metastatic Bone Pain. *Semin Nucl Med.* 2010;40:89-104.
 4. Tsuya A, Fukuoka MJ. Bone metastases in lung cancer. *Clin Calcium.* 2008;18:455-459.
 5. Meckel M, Kubíček V, Hermann P, et al. A DOTA based bisphosphonate with an albumin binding moiety for delayed body clearance for bone targeting. *Nucl Med Biol.* 2016;43:670-678.
 6. Xu Q, Zhang S, Zhao Y, et al. Radiopharmaceuticals. Radiolabeling, quality control, biodistribution, and imaging studies of ¹⁷⁷Lu-ibandronate. *J Labelled Comp Radiopharm.* 2019;62:43-51.
 7. Ayati N, Aryana K, Jalilian A, et al. Treatment efficacy of ¹⁵³Sm-EDTMP for painful bone metastasis. *Asia Oceania Journal of Nuclear Medicine and Biology.* 2013;1:27-31.
 8. Florimonte L, Dellavedova L, Maffioli LS. Radium-223 dichloride in clinical practice: a review. *Eur J Nucl Med Mol Imaging.* 2016;43:1896-909.
 9. Liepe K. ¹⁸⁸Re-HEDP therapy in the therapy of painful bone metastases. *World J Nucl Med.* 2018;17:133-8.
 10. Lepareur N, Lacœuille F, Bouvry C, et al. Rhenium-188 Labeled Radiopharmaceuticals: Current Clinical Applications in Oncology and Promising Perspectives. *Front Med.* 2019;6:132.
 11. Sharma R, Kumar C, Mallia MB, et al, In Vitro Evaluation of ¹⁸⁸Re-HEDP: A Mechanistic View of Bone Pain Palliations. *Cancer Biother Radiopharm.* 2017;32:184-191.
 12. Palmedo H, Guhlke S, Bender H, et al. Dose escalation study with rhenium-188 hydroxyethylidene diphosphonate in prostate cancer patients with osseous metastases. *Eur J Nucl Med.* 2000;27:123-30.
 13. Erfani M, Rahmani N, Doroudi A, et al. Preparation and evaluation of rhenium-188-pamidronate as a palliative treatment in bone metastasis. *Nucl Med Biol.* 2017;49:1-7.
 14. Kucukzeybek Y, Gorumlu G, Cengiz E, et al. Bisphosphonate (Zoledronic Acid) Associated Adverse Events: Single Center Experience. *UHOD.* 2010;20:135-140.
 15. Diel IJ, Weide R, Köppler H, et al. Risk of renal impairment after treatment with ibandronate versus zoledronic acid: a retrospective medical records review. *Support Care Cancer.* 2009;17:719-25.
 16. Weide R, Köppler H, Antras L, et al. Renal toxicity in patients with multiple myeloma receiving zoledronic acid vs. ibandronate: a retrospective medical records review. *J Cancer Res Ther.* 2010;6:31-5.
 17. Meattini I, Bruni A, Scotti V, et al. Oral ibandronate in metastatic bone breast cancer: the Florence University experience and a review of the literature. *J Chemother.* 2010;22:58-62.
 18. Han J, Han L, Zhang L, et al. Comparison of clinical effect in treatment of bone tumor between zoledronic acid needle and ibandronate needle. *Park J Pharm Sci.* 2018;31:1683-1686.
 19. Manafi-Farid R, Masoumi F, Divband G, et al. Targeted Palliative Radionuclide Therapy for Metastatic Bone Pain. *J Clin Med.* 2020;9:2622.
 20. Hashimoto K, Bagiawati S, Izumo M, et al. Synthesis of ¹⁸⁸Re-MDP complex using carrier-free ¹⁸⁸Re. *App Radiat Isot.* 1996;47:195-9.
 21. El-Mabhough AA, Mercer JR. ¹⁸⁸Re-labelled gemcitabine/bisphosphonate (Gem/BP): a multi-functional, bone-specific agent as a potential treatment for bone metastases. *Eur J Nucl Med Mol Imaging.* 2008;35:1240-8.

22. Maxon HR, Schroder LE, Washburn LC, et al. Rhenium-188(Sn)HEDP for treatment of osseous metastases. *J Nucl Med.* 1998;39:659-63.
23. Hsieh BT, Hsieh JF, Tsai SC, et al. Comparison of various rhenium-188-labeled diphosphonates for the treatment of bone metastases. *Nucl Med Biol.* 1999;26:973-976.
24. Verdera ES, Gaudio J, Leon A, et al. Rhenium-188-HEDP-kit Formulation and Quality Control. *Radiochim Acta.* 1997;79:113-8.
25. Nassar MY, El-Kolaly MT, Mahran MRH. Synthesis of a ^{188}Re -HEDP complex using carrier-free ^{188}Re and a study of its stability and biological distribution. *Radiochemistry.* 2011;53:415-420.
26. Oh SJ, Won KS, Moon DH, et al. Preparation and biological evaluation of ^{188}Re -ethylenediamine-N,N',N'-tetrakis(methylene phosphonic acid) as a potential agent for bone pain palliation. *Nucl Med Commun.* 2002;23:75-81.
27. Faintuch BL, Faintuch S, Muramoto E. Complexation of ^{188}Re -phosphonates: in vitro and in vivo studies. *Radiochim Acta.* 2003;91:607-12.
28. Nassar MY, El-Kolaly MT, Mahran MRH. Synthesis of a ^{188}Re -DTPMP complex using carrier-free ^{188}Re and study of its stability. *J Radioanal Nucl Chem.* 2011;287:779-85.
29. Chen LC, Lee WC, Ho CL, et al. Biodistribution, Pharmacokinetics and Efficacy of $^{188}\text{Re}(\text{I})$ -Tricarbonyl-Labeled Human Serum Albumin Microspheres in an Orthotopic Hepatoma Rat Model. *In Vivo.* 2018;32:567-573.
30. Park JY, Lee TS, Choi TH, et al. A comparative study of $^{188}\text{Re}(\text{V})$ -meso-DMSA and $^{188}\text{Re}(\text{V})$ -rac-DMSA: preparation and in vivo evaluation in nude mice xenografted with a neuroendocrine tumor. *Nucl Med Biol.* 2007;34:1029-36.

Tables

Table 2. The biodistribution of [^{188}Re]Re-IBA in mice (n=4)

Tissue	%ID/g (%)					
	1 h	3 h	6 h	8 h	24 h	48 h
Heart	0.568±0.165	0.249±0.021	0.216±0.027	0.159±0.059	0.038±0.009	0.018±0.009
Liver	0.846±0.209	0.498±0.049	0.418±0.079	0.425±0.176	0.098±0.053	0.051±0.017
Spleen	0.788±0.253	0.332±0.074	0.350±0.060	0.383±0.177	0.101±0.072	0.036±0.031
Lung	1.479±0.512	0.659±0.118	0.477±0.092	0.372±0.155	0.108±0.074	0.054±0.055
Kidney	5.391±2.388	2.774±0.374	2.414±0.340	2.094±0.820	0.682±0.033	0.267±0.094
Stomach	2.426±0.239	2.692±0.681	1.401±1.051	1.253±0.830	0.075±0.015	0.029±0.010
Small intestine	0.623±0.412	0.463±0.203	0.597±0.355	0.400±0.112	0.056±0.035	0.028±0.023
Blood	1.574±0.870	0.622±0.103	0.452±0.166	0.325±0.135	0.049±0.016	0.017±0.016
Brain	0.063±0.010	0.049±0.015	0.039±0.016	0.061±0.024	0.019±0.020	0.012±0.018
Femur	6.498±2.534	7.693±2.710	10.394±3.85	6.835±4.159	6.638±3.419	5.699±1.331
Muscle	0.477±0.161	0.242±0.180	0.194±0.091	0.097±0.022	0.045±0.060	0.020±0.027
Gonad	0.923±1.041	0.403±0.151	0.216±0.122	0.189±0.089	0.047±0.024	0.032±0.027
Femur/Heart	11.432	30.908	48.055	42.939	174.255	327.902
Femur/Liver	7.677	15.422	24.843	16.071	68.036	111.183
Femur/Blood	4.128	12.365	23.014	21.026	135.907	326.053
Femur/Muscle	13.611	31.736	53.560	70.632	146.875	291.551

*The percentage injection dose rate per gram of tissue (%ID/g) is expressed as mean±standard deviation ($\bar{x}\pm s$).

Table 3. The biodistribution of [^{188}Re]ReO $_4^-$ in mice (n=4)

Tissue	%ID/g (%)					
	1 h	3 h	6 h	8 h	24 h	48 h
Heart	1.422±0.339	0.401±0.050	0.176±0.074	0.084±0.030	0.017±0.005	0.011±0.004
Liver	2.480±0.556	0.530±0.038	0.258±0.086	0.132±0.024	0.023±0.010	0.018±0.010
Spleen	2.341±0.973	0.490±0.090	0.270±0.098	0.117±0.041	0.028±0.007	0.022±0.006
Lung	4.458±1.379	1.026±0.312	0.487±0.132	0.307±0.180	0.054±0.017	0.036±0.008
Kidney	2.923±0.658	0.683±0.118	0.338±0.191	0.132±0.053	0.017±0.003	0.017±0.007
Stomach	22.747±5.67	8.578±3.928	2.828±1.287	1.760±1.006	0.053±0.032	0.029±0.012
Small intestine	1.671±0.448	0.558±0.207	0.263±0.050	0.177±0.033	0.023±0.004	0.014±0.005
Blood	4.648±1.631	1.578±0.419	0.533±0.254	0.221±0.043	0.023±0.009	0.007±0.002
Brain	0.207±0.044	0.070±0.024	0.044±0.019	0.015±0.008	0.017±0.004	0.013±0.006
Femur	1.670±0.345	0.431±0.038	0.213±0.102	0.105±0.025	0.031±0.003	0.011±0.005
Muscle	0.775±0.074	0.182±0.023	0.109±0.065	0.038±0.010	0.021±0.008	0.020±0.005
Gonad	1.096±0.007	0.404±0.130	0.207±0.065	0.061±0.037	0.021±0.009	0.007±0.001
Femur/Heart	1.195	1.075	1.205	1.255	1.853	1.060
Femur/Liver	0.685	0.813	0.823	0.797	1.325	0.638
Femur/Blood	0.366	0.273	0.399	0.477	1.359	1.650
Femur/Muscle	2.193	2.372	1.950	2.762	1.498	0.585

*The percentage injection dose rate per gram of tissue (%ID/g) is expressed as mean±standard deviation ($\bar{x}\pm s$).

Figures

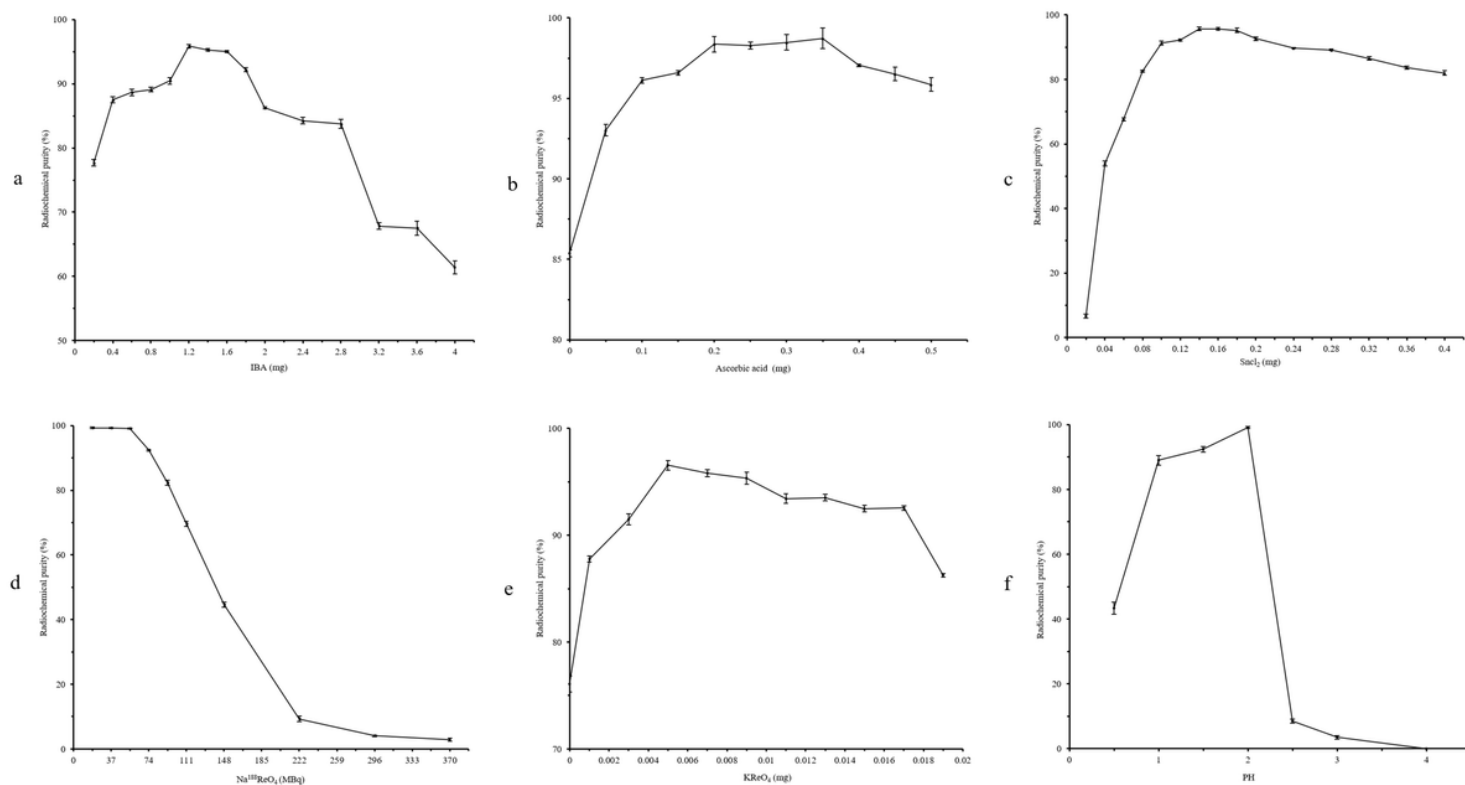


Figure 1

Effects of various reaction parameters on the radiochemical purity of $[^{188}\text{Re}]\text{Re-IBA}$. The optimal proportion and condition for the production of $[^{188}\text{Re}]\text{Re-IBA}$ were as follows: IBA, 1.2–1.6 mg (a); ascorbic acid, 0.20–0.35 mg (b); SnCl_2 , 0.14–0.18 mg (c); $[^{188}\text{Re}]\text{ReO}_4^-$ activity, 18.5–55 MBq (d); KReO_4 , 0.005–0.009 mg (e); and pH = 2 (f).

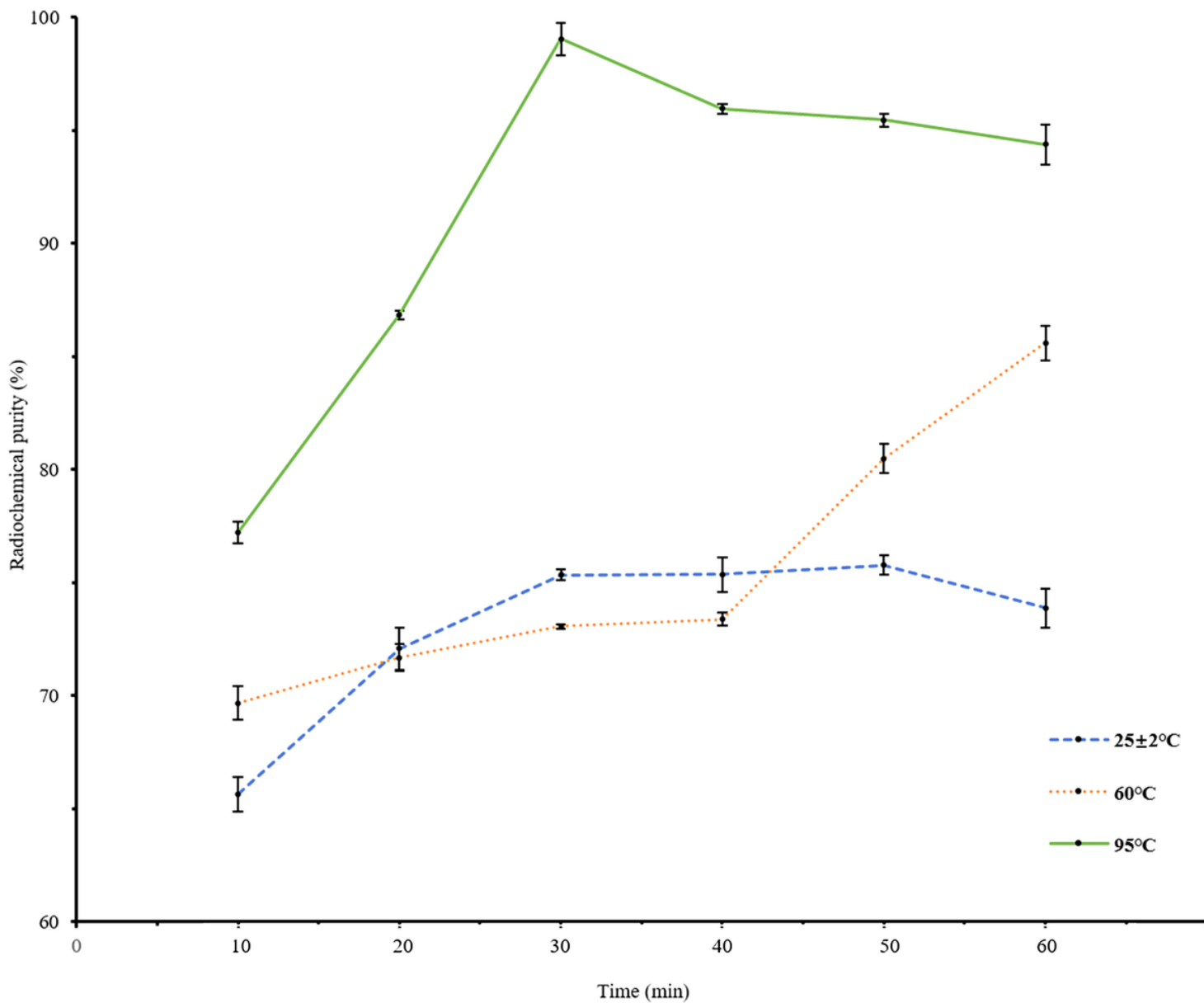


Figure 2

The effect of temperature and reaction time on the radiochemical purity of $[^{188}\text{Re}]\text{Re-IBA}$. The optimal temperature and reaction for the production of $[^{188}\text{Re}]\text{Re-IBA}$ was reacted for 30min at 95 °C.

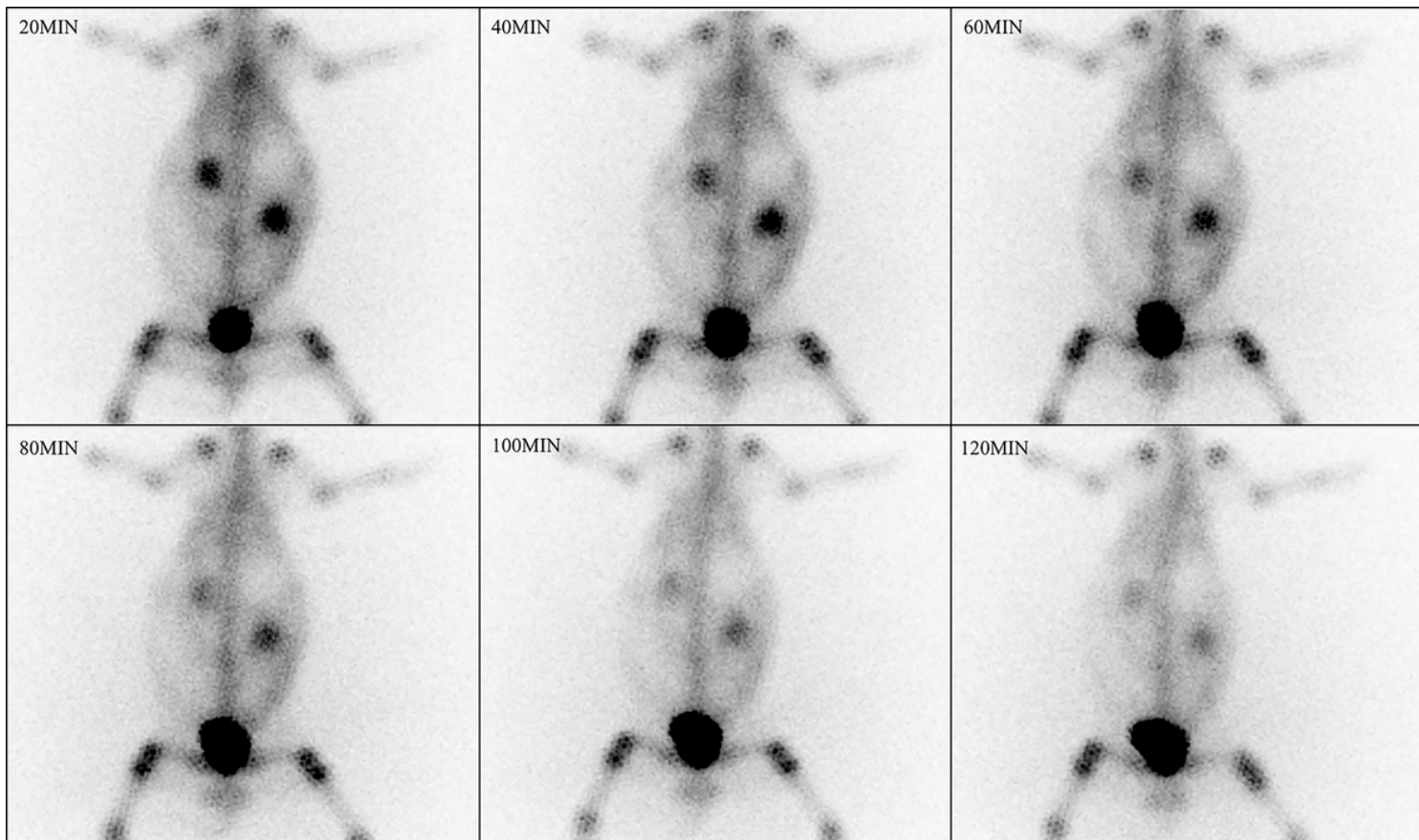


Figure 3

Dynamic bone imaging (20–120 min) in New Zealand rabbits. There was an obvious accumulation in both kidneys, bladder, and bones at 20 min after the injection. As time goes on, the accumulation in the kidneys gradually faded and got into the bladder, and bone imaging gradually clearer.

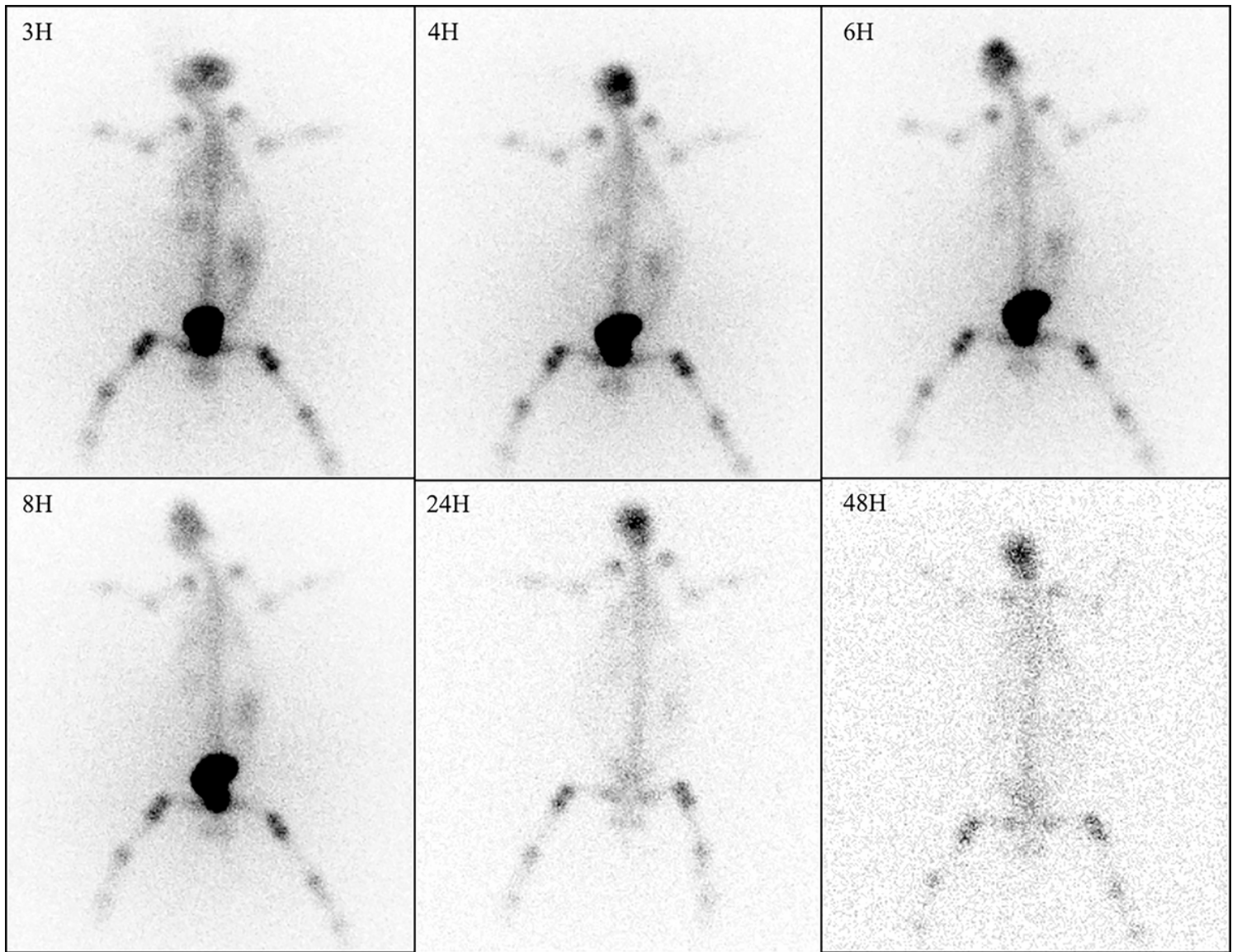


Figure 4

Whole-body bone static imaging (3–48 h) in New Zealand rabbits. There was an obvious accumulation in bones at 3–48 h after the injection, and the whole-body bone imaging was clear with a high contrast between the bone and the background. Furthermore, the uptake of liver, spleen, and soft tissue was low.